

New Phytologist Supporting Information

Article title:

Tomato geranylgeranyl diphosphate synthase isoform 1 is involved in the stress-triggered production of diterpenes in leaves and strigolactones in roots

Authors:

Miguel Ezquerro, Changsheng Li, Julia Pérez-Pérez, Esteban Burbano-Erazo, M. Victoria Barja, Yanting Wang, Lemeng Dong, Purificación Lisón, M. Pilar López-Gresa, Harro J. Bouwmeester, Manuel Rodríguez-Concepción

Article acceptance date: 5 June 2023

The following Supporting Information is available for this article:

Methods S1. Metabolite analyses.

Methods S2. Gene expression analyses.

Methods S3. Co-immunoprecipitation assays.

Fig. S1. DNA sequence alignment of *SIG1* CRISPR mutants.

Fig. S2. Protein alignments of *SIG1* wild-type sequences with the selected CRISPR mutants.

Fig. S3. *SIG1*, *SIG2* and *SIG3* transcript levels in different tissues and developmental stages.

Fig. S4. Expression levels of genes encoding GLS and GGPPS isoforms in leaves after *Pseudomonas syringae* infection.

Fig. S5. *SIG1*-Myc is able to specifically bind to protein partners.

Fig. S6. Root parameters in SL-defective mutants.

Table S1. List of primers used in this work.

Table S2. Constructs and cloning details.

Table S3. Co-expression of tomato GGPPS paralogs (guide genes) with isoprenoid-related genes (query genes) in root tissue.

SUPPORTING METHODS

Methods S1. Metabolite analyses.

Isoprenoid extraction and quantification. Carotenoids, chlorophylls and tocopherols were extracted as described (Barja et al., 2021; Ezquerro et al., 2022) with some modifications. Freeze-dried tissue powder from roots (25 mg) or leaves (8 mg) was mixed in 2 ml Eppendorf tubes with 375 μ l of methanol as extraction solvent, 25 μ l of a 10 % (w/v) solution of canthaxanthin (Sigma) in chloroform as internal control, and three 2 mm glass beads. In the case of pericarp tissue, freeze-dried powder (20 mg) was 1 ml of 2:1:1 hexane:acetone:methanol was used instead of methanol. Following extraction as described (Barja et al., 2021; Ezquerro et al., 2022), dry residues were resuspended in 200 μ l of acetone by using an ultrasound bath and filtered with 0.2 μ m filters into amber-colored 2 ml glass vials. Separation and quantification of individual carotenoids, chlorophylls and tocopherols was performed as described (Barja et al., 2021).

ABA extraction and quantification. For ABA quantification, 20 mg of freeze-dried root powder was mixed using 1 ml of 10% methanol in water (containing internal ABA standard) by shaking in a TissueLyser II (Quiagen) at 27 Hz for 3 min. Next, samples were placed in a rotator for 1 hour at 4°C. Extracts were then centrifuged at 14000 xg at 4°C for 15 min. Around 800 μ l of the liquid phase was recovered in 1.5 ml Eppendorf for further steps. Eluted liquid was run through an Oasis HLB (reverse phase) column as described (Flokova et al., 2014). The dry residues were dissolved in 1 ml of pure methanol and after, dried under a nitrogen flow in a fume hood for 40 min. The eluate was dissolved in 5% acetonitrile and ABA was detected using a reverse phase UHPLC chromatography. The gradient used contains 5 to 50% acetonitrile with 0.05% acetic acid, at a flow speed of 400 μ L/min over 21 min. Quantification of ABA was performed with a Q-Exactive mass spectrometer (Orbitrap detector; ThermoFisher Scientific) in conjunction with internal standards (deuterium-labelled hormone at 1pmol/ μ l), calibration curves and the TraceFinder 4.1 SP1 software.

SL extraction and quantification. Tomato seedlings growing in a mixture of river sand and a clay granulate (1:1) were supplied with half-strength Hoagland solution twice a week for 28 days. After 28 days, plants were divided into two groups of which one continued to get the half-strength Hoagland solution for 7 days, while the other was exposed to phosphorus deficiency (by using half-strength Hoagland solutions without phosphate) to induce SL biosynthesis and exudation. Pots were washed with 100 ml of sterile milli-Q water to collect the SLs, which were then concentrated using C18 SPE columns (SUPELCO, Discovery® DSC-18 SPE, 500 mg/3 mL) and analyzed by LC-MS/MS as described (Zhang et al., 2014; 2018). Identification of individual SLs was based on earlier publications on tomato SLs, using authentic standards of solanacol, orobanchol, oxo-orobanchol and tentatively identified hydroxyl-orobanchol, kindly provided by Koichi Yoneyama (Xie et al., 2009; Kohlen et al., 2012; Wang et al., 2022).

Analysis of volatile organic compounds. For the analysis of VOCs, frozen tomato leaf powder (150 mg) was mixed in a 15 ml glass vial with 1 mL of a saturated CaCl_2 solution and 100 μL of 750 mM EDTA (pH 7.5). The vial was sealed and sonicated for 5 min and volatile compounds extraction was performed by Head Space Solid-Phase Microextraction (HS-SPME) as previously reported (López-Gresa et al., 2017). VOCs were analyzed in an Agilent 6890N (Santa Clara, CA, USA) gas chromatograph coupled to an Agilent 5975B Inert XL electronic impact (EI) mass detector with an ionization energy of 70 eV and a source temperature of 300°C. Chromatograms were processed using the Enhanced ChemStation software (Agilent). Final identification of and quantification of GL was performed using a commercial standard (Sigma).

Methods S2. Gene expression analyses.

Gene co-expression network (GCN) analyses. The data set used for Gene co-expression network construction was previously described (Wang et al., 2021) and it is publicly available in <https://dataview.ncbi.nlm.nih.gov/object/PRJNA679261?reviewer=vs5lk0a94j04c2rgieta1lrlro>. It is composed by tomato root samples grown in +P and -P conditions. Tomato isoprenoid biosynthetic genes were retrieved from Plaza 4.0 using Arabidopsis homologs as queries (<https://bioinformatics.psb.ugent.be/plaza/>) as previously described (Wang et al., 2022). Pairwise Pearson correlation coefficients (PCC) were calculated between every two genes using *SIG1*, *SIG2* and *SIG3* as baits and tomato isoprenoid biosynthetic genes as preys. Figures were constructed using R software (<https://www.r-project.org/>).

RNA extraction and RT-qPCR analyses. Total RNA from freeze-dried leaves and roots was extracted using TriPure isolation reagent (Sigma) combined with a Qiagen RNeasy mini spin column kit following manufacturer's instructions. RNA was quantified using a NanoDrop™ 8000 spectrophotometer (ThermoFisher Scientific). ThermoFisher First Strand cDNA synthesis kit using oligo(dT) primer was used to reverse transcribe 1000 ng of RNA into 20 μL of cDNA, which was subsequently diluted 10-fold with milli-Q water and stored at -20 °C for further analysis. Relative mRNA abundance was evaluated via Real-Time Quantitative Polymerase Chain Reaction (RT-qPCR) in a reaction volume of 10 μL containing 5 μL of SYBR Green Master Mix (Thermo Fisher Scientific), 0.3 μM of each specific forward and reverse primer (Table S1) and 2 μL of cDNA. Transcript abundance was evaluated via real-time quantitative PCR (RT-qPCR) in a reaction volume of 10 μL containing 2 μL of the cDNA dilution, 5 μL of SYBR Green Master Mix (Thermo Fisher Scientific), and 0.3 μM of each specific forward and reverse primer (Table S1). The RT-qPCR was carried out on a QuantStudio 3 Real-Time PCR System (Thermo Fisher Scientific) using three independent biological samples and three technical replicates of each sample. Normalized transcript abundance was calculated as previously described (Simon, 2003) using tomato *ACT4* (Solyc04g011500) as endogenous reference gene.

Methods S3. Co-immunoprecipitation assays.

Co-immunoprecipitation experiments were carried out as described (Barja & Rodríguez-Concepción, 2020; Barja et al., 2021) (Methods S3). Constructs encoding Myc- and HA-tagged tomato GGPPS and PSY proteins (Table S2) (Barja et al., 2021) were transformed into *A. tumefaciens* GV3101 strains. A plasmid containing the Arabidopsis phosphoribulokinase protein with a Myc tag (pGWB417_PRK-Myc) was used as negative control. Agroinfiltration of *N. benthamiana* leaves, sample collection, protein extraction and immunoprecipitation of proteins was performed as described (Barja et al., 2021). Myc- and HA-tagged proteins in input and Co-IP samples were detected by immunoblot analyses using 1:2000 α Myc (Sigma) and 1:1000 α HA (Roche) dilutions. Horseradish peroxidase (HRP)-conjugated secondary antibodies against mouse and rat IgGs, respectively were used in a 1:10000 dilution. Amersham ECL Prime Western Blotting Detection Kit (GE Healthcare) was used for detection and the signal was visualized using the Amersham ImageQuant 800 Western blot imaging system.

SUPPORTING FIGURES

Figure S1. DNA sequence alignment of *SLG1* CRISPR mutants. Alignment was performed using Clustal Omega (<https://www.ebi.ac.uk/Tools/msa/clustalo/>) with default settings. The sequence encoding the predicted plastid-targeting peptide is marked in green. Designed single-guide RNAs (sgRNA) are highlighted in blue and genotyping oligonucleotides are highlighted in fuchsia. Protospacer adjacent motifs (PAM) are highlighted in red. Translation stop codons are underlined and marked in bold. Numbers at the end of each sequence indicate DNA sequence length.

```

SLG1      ATGGCATTTTTAGCTACCATTTCTGGCCTTGACAATCTGTTTCCTTTCTAATACCCCAAAC 60
slg1-1   ATGGCATTTTTAGCTACCATTTCTGGCCTTGACAATCTGTTTCCTTTCTAATACCCCAAAC 60
slg1-2   ATGGCATTTTTAGCTACCATTTCTGGCCTTGACAATCTGTTTCCTTTCTAATACCCCAAAC 60
*****

SLG1      ATAAACTTTGCTTTCAGTAGAAAACTCCACCAAGCCAATCTTACAGTTTCCTTCACAAG 120
slg1-1   ATAAACTTTGCTTTCAGTAGAAAACTCCACCAAGCCAATCTTACAGTTTCCTTCACAAG 120
slg1-2   ATAAACTTTGCTTTCAGTAGAAAACTCCACCAAGCCAATCTTACAGTTTCCTTCACAAG 120
*****

SLG1      AAAATAACGCTAGCGATGTTGCGAACTCGTTCCAACTTTTCAAGTCAAGGAACGAGAT 180
slg1-1   AAAATAACGCTAGCGATGTTGCGAACTCGTTCCAACTTTTCAAGTCAAGGAACGAGAT 180
slg1-2   AAAATAACGCTAGCGATGTTGCGAACTCGTTCCAACTTTTCAAGTCAAGGAACGAGAT 180
*****

SLG1      GTTTCATCCAAGGCAGAGAAATTCATCTTGCCTGAGTTTGAGTTTCAAGAATACATGGTA 240
slg1-1   GTTTCATCCAAGGCAGAGAAATTCATCTTGCCTGAGTTTGAGTTTCAAGAATACATGGTA 240
slg1-2   GTTTCATCCAAGGCAGAGAAATTCATCTTGCCTGAGTTTGAGTTTCAAGAATACATGGTA 240
*****

SLG1      ACGAAGGCAATCAAGGTAAACAAAGCACTAGATGAAGCAATACCAATGCAAGAGCCTATA 300
slg1-1   ACGAAGGCAATCAAGGTAAACAAAGCACTAGATGAAGCAATACCAATGCAAGAGCCTATA 300
slg1-2   ACGAAGGCAATCAAGGTAAACAAAGCACTAGATGAAGCAATACCAATGCAAGAGCCTATA 300
*****

SLG1      AAAGTTCATGAAGCCATGAGGTACTCACTTCTAGCTGGAGGAAAACGTGTCCGGCCGATC 360
slg1-1   AAAGTTCATGAAGCCATGAGGTACTCACTTCTAGCTGGAGGAAAACGTGTCCGGCCGATC 360
slg1-2   AAAGTTCATGAAGCCATGAGGTACTCACTTCTAGCTGGAGGAAAACGTGTCCGGCCGATC 360
*****

SLG1      CTCTGCATGGCTTCTTGTGAAGTTGTAGGAGGGGATGAATCCTTAGCTATACCTGCAGGCT 420
slg1-1   CTCTGCATGGCTTCTTGTGAAGTTGTAGGAGGGGATGAATCCTTAGCTATACCTGCAGGCT 420
slg1-2   CTCTGCATGGCTTCTTGTGAAGTTGTAGGAGGGGATGAATCCTTAGCTATACCTGCAGGCT 420
*****

G1 CRISPR Geno F
SLG1      TGCGCAGTTGAGATGATCCATACCATGTCACCTCGTCCATGATGATCTTCCCTGCATGGAC 480
slg1-1   TGCGCAGTTGAGATGATCCATACCATGTCACCTCGTCCATGATGATCTTCCCTGCATGGAC 480
slg1-2   TGCGCAGTTGAGATGATCCATACCATGTCACCTCGTCCATGATGATCTTCCCTGCATGGAC 480
*****

SLG1      AACGATGATCTACGTCGTGGCAAGCCACGAACCATAAGGTTTTTGGAGAAAACACTGCA 540
slg1-1   AACGATGATCTACGTCGTGGCAAGCCACGAACCATAAGGTTTTTGGAGAAAACACTGCA 540
slg1-2   AACGATGATCTACGTCGTGGCAAGCCACGAACCATAAGGTTTTTGGAGAAAACACTGCA 540
*****

SLG1      GTTCTTGCAAGGGGATGCACTTTTATCTTTGGCCTTTGAACATGTGGCTACCAAGACTCAG 600
slg1-1   GTTCTTGCAAGGGGATGCACTTTTATCTTTGGCCTTTGAACATGTGGCTACCAAGACTCAG 600
slg1-2   G----- 541
*

```

sgRNA-1

SLG1 AATGTGCCACCCCAAAGAGTGGTCCAAGCCATTGGGGAATTGG**G TTCAGCTGTTGGCTCA** 660
 slg1-1 AATGTGCCACCCCAAAGAGTGGTCCAAGCCATTGGGGAATTGGGTT**CAGCTGTTGGCTCA** 660
 slg1-2 -----541

PAM

SLG1 **GAA**GGGCTCGTGGCAGGGCAAATTGTGGACTTGGCGAGTGAAGGAAAACAAGTTAGCCTA 720
 slg1-1 GAAGGGCTCGTGGCAGG----- 677
 slg1-2 ----- 541

sgRNA-2 PAM

SLG1 ACTGAACTGGAG**GTACATTCACCACCATAAGA**CGGCGAAGCTTTTGGAGGCTGCTGTGGTT 780
 slg1-1 ----- 677
 slg1-2 ----- 541

SLG1 TGTGGGGCAATAATGGGGGAGGAAATGAGGTTGATGTGGAGCGAATGAGGAGCTATGCT 840
 slg1-1 ----- 677
 slg1-2 ----- 541

SLG1 AGGTGCATTGGACTGTTATTTCAAGTGGTAGATGATATTCTTGATGTTACCAAGTCATCA 900
 slg1-1 ----- 677
 slg1-2 -----TTCTTGATGTTACCAAGTCATCA 569

SLG1 GATGAGCTGGGAAAGACAGCGGGTAAGGACCTAATAACAGATAAGGCTACATATCCTAAG 960
 slg1-1 -----G**TAA**GGACCTAATAACAGATAAGGCTACATATCCTAAG 715
 slg1-2 GATGAGCTGGGAAAGACAGCGGGTAAGGACCTAATAACAGATAAGGCTACATATCCTAAG 644

G1 CRISPR Geno R

SLG1 TT**GATGGGGCTAGAAAAGGCTC**GACAATATGCCGGTGAGCTGATGGCTAAGGCCATGAAT 1020
 slg1-1 TT**GATGGGGCTAGAAAAGGCTC**GACAATATGCCGGTGAGCTGATGGCTAAGGCCATGAAT 775
 slg1-2 TT**GATGGGGCTAGAAAAGGCTC**GACAATATGCCGGTGAGCTGATGGCTAAGGCCATGAAT 684

SLG1 GAGCTAAGCTACTTCGACTATGCAAAGGCAGCACCTCTTTATCATATTGCTAGTTATATT 1080
 slg1-1 GAGCTAAGCTACTTCGACTATGCAAAGGCAGCACCTCTTTATCATATTGCTAGTTATATT 835
 slg1-2 GAGCTAAGCTACTTCGACTATGCAAAGGCAGCACCTCTTTATCATATTGCTAGTTATATT 744

SLG1 GCAAATCGACAGAAT**TGA** 1098
 slg1-1 GCAAATCGACAGAATTGA 853
 slg1-2 GCAAATCGACAGAAT**TGA** 762

Figure S2. Protein alignments of SIG1 wild-type sequences with the selected CRISPR mutants. Multiple sequence alignment was performed using *Clustal Omega* (<https://www.ebi.ac.uk/Tools/msa/clustalo/>) with default settings. The predicted targeting peptides, the region of the designed sgRNAs and the catalytic motifs FARM (first aspartate-rich motif) and SARM (second-aspartate rich motif) are boxed in green, blue and black, respectively. The protein-protein interaction CxxxC (x = any hydrophobic residue) motifs are highlighted in pink. Numbers at the end of each sequence indicate protein length.

	Transit peptide	
Slg1	MAFLATISGLDNLFLSNTPNNNFAFSRKLPPSQSYSFLHKKIH	ASDVANSFQTFQVKERD 60
slg1-1	MAFLATISGLDNLFLSNTPNNNFAFSRKLPPSQSYSFLHKKIH	ASDVANSFQTFQVKERD 60
slg1-2	MAFLATISGLDNLFLSNTPNNNFAFSRKLPPSQSYSFLHKKIH	ASDVANSFQTFQVKERD 60

Slg1	VSSKA EKFILPEFEFQEYMTKAIKVNKALDEAIPMQEPIKVHEAMRYSLLAGGKRV RPI	120
slg1-1	VSSKA EKFILPEFEFQEYMTKAIKVNKALDEAIPMQEPIKVHEAMRYSLLAGGKRV RPI	120
slg1-2	VSSKA EKFILPEFEFQEYMTKAIKVNKALDEAIPMQEPIKVHEAMRYSLLAGGKRV RPI	120

	CxxxC	FARM
Slg1	L <b style="color: magenta;">CMASCE EVVGGDESLAIPAAVAVEMIH TMSLVH	<b style="background-color: black; color: black;">DDLPCMD NDDLRRGKPTNHKVF GENTA 180
slg1-1	L <b style="color: magenta;">CMASCE EVVGGDESLAIPAAVAVEMIH TMSLVH	<b style="background-color: black; color: black;">DDLPCMD NDDLRRGKPTNHKVF GENTA 180
slg1-2	L <b style="color: magenta;">CMASCE EVVGGDESLAIPAAVAVEMIH TMSLVH	<b style="background-color: black; color: black;">DDLPCMD NDDLRRGKPTNHKVF GENTA 180

		sgRNA-1
Slg1	VLAGDALLSLAFEHVATKTQNVPPQRVVQAIGELG	<b style="background-color: #ADD8E6;">SAVGSEGL VAGQIVDLASEGKQVSL 240
slg1-1	VLAGDALLSLAFEHVATKTQNVPPQRVVQAIGELG	<b style="background-color: #ADD8E6;">SAVGSEGL VAG*----- 226
slg1-2	V-----	----- 181
*		
	sgRNA-2	SARM
Slg1	TELE <b style="background-color: #ADD8E6;">YIHHHKTA KLLEAAVVCGAIMG GNEVDVERMRSYARCIGLLFQVV	<b style="background-color: black; color: black;">DDILD VTKSS 300
slg1-1	-----	----- 226
slg1-2	-----	----- <b style="background-color: black; color: black;">LD VTKSS 188
Slg1	DELGKTAGKDLITDKATYPKLMGLEKARQYAGELMAKAMNELSYFDYAKAAPLYHIAS YI	360
slg1-1	-----	----- 226

Figure S3. *SIG1*, *SIG2* and *SIG3* transcript levels in different tissues and developmental stages.

(a) RNAseq data retrieved from the *Tomato eFP Browser* database (http://bar.utoronto.ca/efp_tomato/cgi-bin/efpWeb.cgi). Levels are represented as RPKM (Reads per Kilobase of transcript per Million mapped reads). **(b)** RNAseq data obtained from Genevestigator (<https://genevestigator.com>). Levels are represented as log₂ TPM (Transcripts Per Million mapped reads). Abbreviations: DPA, days post-anthesis; IG, immature green; MG, mature green; B, breaker; O, orange, R, red. YL, young leaves; ML, mature leaves.

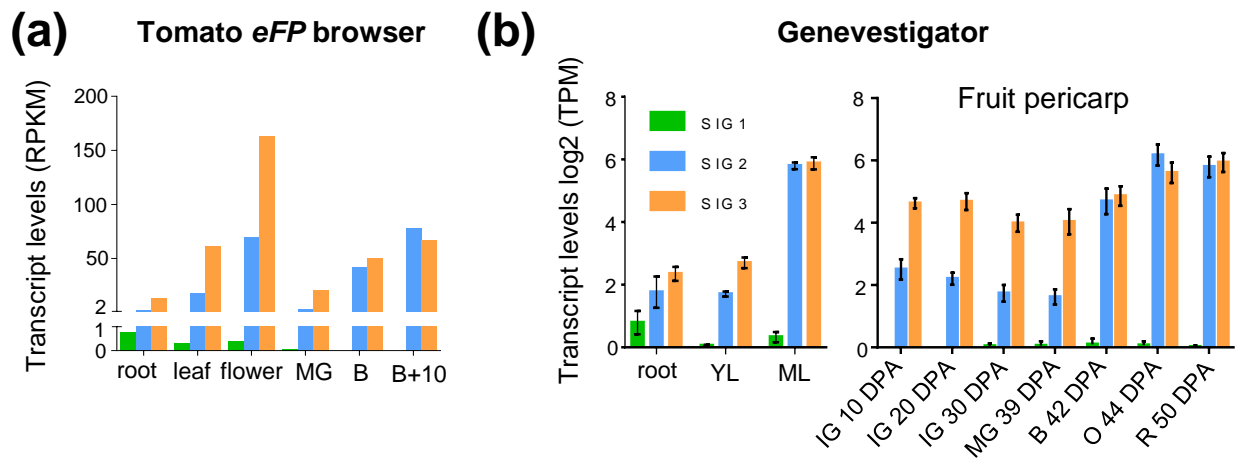


Figure S4. Expression levels of genes encoding GLS and GGPPS isoforms in leaves after *Pseudomonas syringae* infection. RNAseq data obtained from Genevestigator (<https://genevestigator.com>) of three different tomato infection experiments with *P. syringae* pv. *tomato* DC3000, using samples collected at 9 (Ailsa Craig) or 6 (Rio Grande) hours post infection. Plots show the transcript levels of the indicated genes in leaves of both cultivars during *P. syringae* pv. *tomato* DC3000 infection and are shown as log₂ TPM (Transcripts per Million mapped reads).

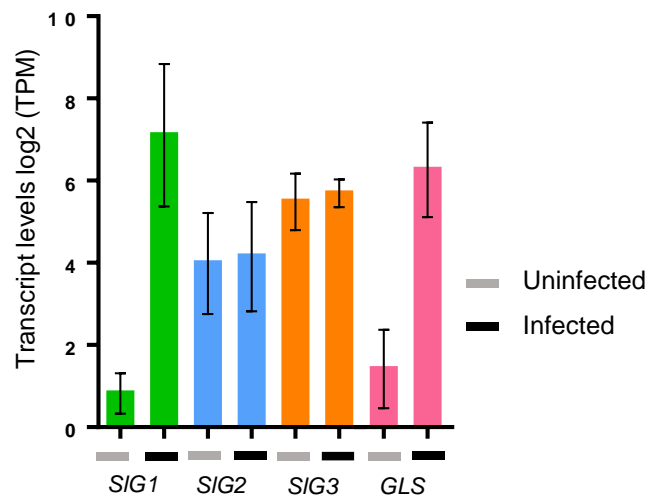
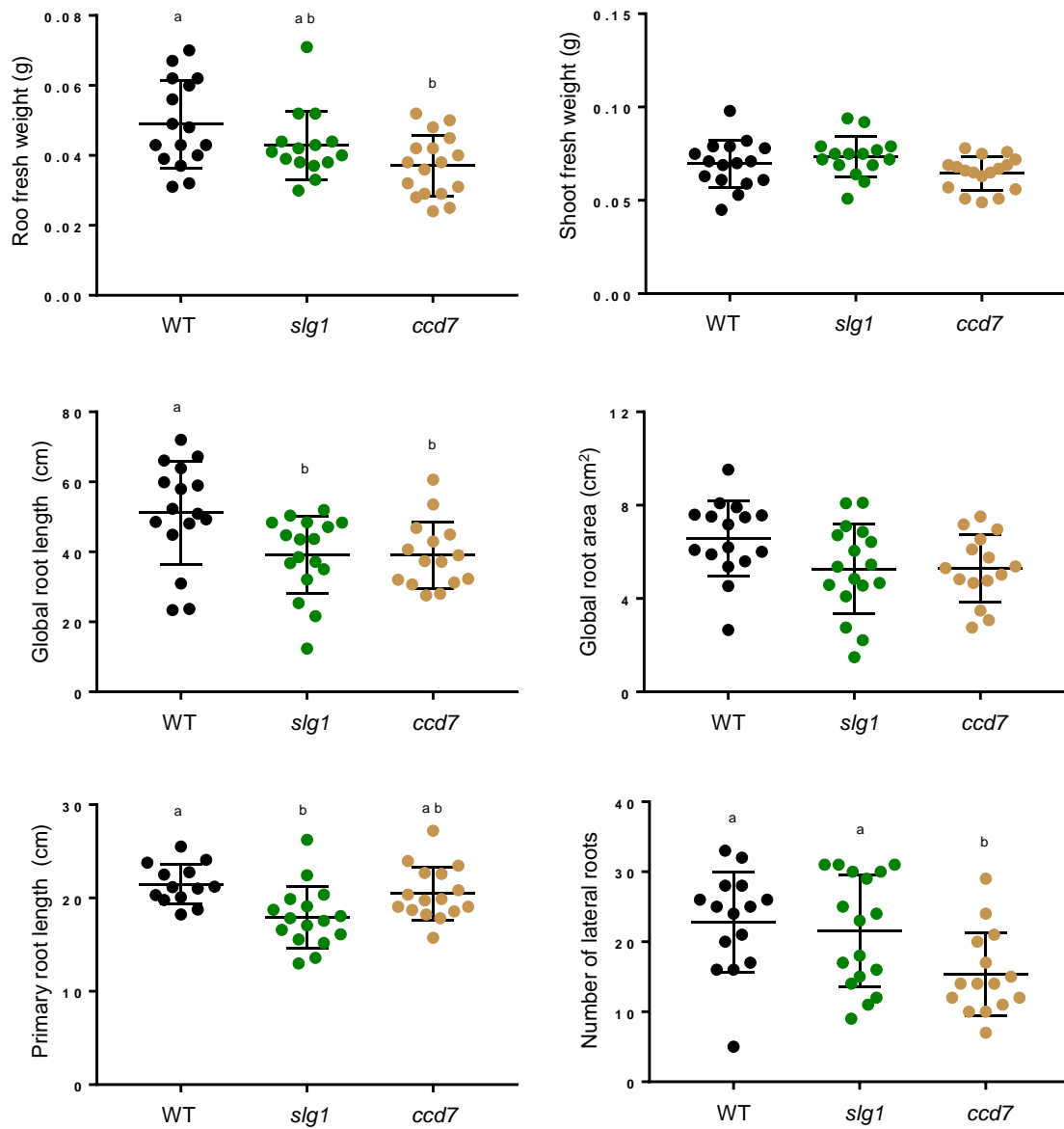


Figure S6. Root parameters in SL-defective mutants. WT, *slg1-1* and *ccd7* lines were germinated and grown for two weeks on vertical plates with solid medium lacking P. The lower section of the dishes was covered with aluminum foil so only the shoots were directly exposed to light. Individual measurements (colored dots) and well as mean and SD of the indicated parameters are shown. In all plots, letters represent statistically significant differences ($P < 0.05$) among means according to post hoc Tukey's tests run when one way ANOVA detected different means.



SUPPORTING TABLES

Table S1. List of primers used in this work.

Use	Name	Sequence (5'-3') ¹
Cloning	SIG1-attB1-F	GGG GACAAGTTTGTACAAAAAAGCAGGCT GG ATGGCATTTTTAGCTACCATTCTG
	SIG1-attB2-R	GGG GACCACCTTTGTACAAGAAAGCT GGG TGATTCTGTTCGATTTGCAATATAACTAGC
	SIPSY3-attB1-F	GGG GACAAGTTTGTACAAAAAAGCAGGCT GG ATGTGTCCAGCAACACTTTCTTATT
	SIPSY3-attB2-R	GGG GACCACCTTTGTACAAGAAAGCT GGG TGTTGAATGGCTAAACTAGGCCAAAGATAAAG
	AtPRK-attB1-F	GGG GACAAGTTTGTACAAAAAAGCAGGCTATGGCTGTCTCAACTATCTAC
	AtPRK-attB2-R	GGG GACCACCTTTGTACAAGAAAGCT GGG TGGCTTTAGCTTCTGCACGAGC
RT-qPCR	SIPSY1-qPCR-F	ACAGGCAGGTCTATCCGATG
	SIPSY1-qPCR-R	ACGCCTTTCTCTGCCTCATC
	SIPSY2-qPCR-F	CAGGGCTCTCCGATGAAGAC
	SIPSY2-qPCR-R	CACCGGCCATCTACTAGCAG
	SIPSY3-qPCR-F	TTGGATGCAATAGAGGAGAATG
	SIPSY3-qPCR-R	ATTGAATGGCTAAACTAGGCCAAAG
	SIG1-qPCR-F	GGCCTTTGAACATGTGGCTACC
	SIG1-qPCR-R	ACTCGCCAAGTCCACAATTTGC
	SIG2-qPCR-F	AAAGTCATCGTCGGAGCTCG
	SIG2-qPCR-R	GTTTAGCTTCGCCGTTGAGC
	SIG3-qPCR-F	AGGAGGTGCACCAGATGAAG
	SIG3-qPCR-R	TCAGCAACCAAGTCCTTCCC
	SIGLS-qPCR F	TTGCTCATGACCACAACCTCG
	SIGLS-qPCR R	GGAGCTTCATTGTTCTTGCCA
SIACT4-qPCR-F	CCTTCCACATGCCATTCTCC	
SIACT4-qPCR-R	CCACGCTCGGTCAGGATCT	
sgRNAs for CRISPR-Cas9 gene impairment	SIG1-sgRNA-1 F	ATTGGTTCAGCTGTTGGCTCAGAA
	SIG1-sgRNA-1 R	AAACTTCTGAGCCAACAGCTGAAC
	SIG1-sgRNA-2 F	ATTGGTACATTCACCACCATAAGA
	SIG1-sgRNA-2 R	AAACTCTTATGGTGGTGAATGTAC
CRISPR plants genotyping	SIG1 Geno F	GCTTGCGCAGTTGAGATGATCC
	SIG1 Geno R	GGTCCTTACCCGCTGTCTTTCC
	Cas9 F	TCCCTCATCAGATCCACCTC
	Cas9 R	CTGAAACGTGAGCCTTCTGG
	NTP II F	GAAGGGGATAGAAGGCGA
	NTP II R	AGATGGATTGCACGCAGG

¹Gateway recombination sites in bold

Table S2. Constructs and cloning details.

Use	Construct	Template	Primers ¹	Sequence cloned ²	Cloning method	Entry plasmid	Destiny plasmid	
Co-immunoprecipitation assays	SIG1-HA	Tomato root cDNA	1+2	SIG1 ₁₋₁₀₉₈	Gateway	pDONR207	pGWB414	
	SIPSY1-HA	Tomato fruit cDNA		SIPSY1 ₁₋₁₂₃₆	Gateway	pDONR207	pGWB414	
	SIPSY2-HA	Tomato leaf cDNA		SIPSY2 ₁₋₁₃₁₄	Gateway	pDONR207	pGWB414	
	SIPSY3-HA	Tomato root cDNA	3+4	SIPSY3 ₁₋₁₁₈₆	Gateway	pDONR207	pGWB414	
	SIG1-Myc	Tomato root cDNA	1+2	SIG1 ₁₋₁₀₉₈	Gateway	pDONR207	pGWB420	
	SIG2-Myc	Tomato flower cDNA		SIG2 ₁₋₁₀₈₉	Gateway	pDONR207	pGWB420	
	SIG3-Myc	Tomato flower cDNA		SIG3 ₁₋₁₀₈₀	Gateway	pDONR207	pGWB420	
	AtPRK-Myc	Arabidopsis seedling cDNA	5+6	AtPRK ₁₋₁₅₅₆	Gateway	pDONR207	pGWB417	
	CRISPR-Cas9 gene impairment	pEN-SIG1(<i>sg1</i>)	-	23+24	SIG1 ₆₄₄₋₆₆₄	BbsI / T4 ligase	pENC1.1	-
		pEN-SIG1(<i>sg2</i>)	-	25+26	SIG1 ₇₃₂₋₇₅₂	BbsI / T4 ligase	pENC1.1	-
pDE-SIG1(1+2)		pEN-SIG1(<i>sg1</i>) + (<i>sg2</i>)	-	SIG2 ₆₄₄₋₆₆₄ + SIG2 ₇₃₂₋₇₅₂	(<i>sg1</i>)MluI + Bsu36I / T4 ligase (<i>sg2</i>)Gateway	pEN-SIG1(<i>sg1</i>) + (<i>sg2</i>)	pDE-Cas9	

¹Constructs without primers reported in Barja et al. (2021)

²Numbers indicate the first and last nucleotide positions cloned from the coding sequence of the indicated gene.

Table S3. Co-expression of tomato GGPPS paralogs (guide genes) with isoprenoid-related genes (query genes) in root tissue. Significant pairwise Pearson correlations between guide and query genes (≥ 0.55) are highlighted in red (when positive) or green (when negative). Arabidopsis genes were used as queries in PLAZA 4 to search for tomato homologs (https://bioinformatics.psb.ugent.be/plaza/versions/plaza_v4_dicots/). Genes are organized by pathways.

Pathway/Family	Name	SOL Tomato gene	SIG1	SIG2	SIG3
			Solyc11g011240	Solyc04g079960	Solyc02g085700
MEP pathway	DXS1	Solyc01g067890	0.227817285	-0.432217062	0.28528147
MEP pathway	DXS2	Solyc11g010850	0.997036917	-0.103686573	0.326655343
MEP pathway	DXS3a	Solyc01g028900	0.055742093	-0.087928801	0.718940454
MEP pathway	DXS3b	Solyc08g066950	0.639972045	-0.070017463	0.741305712
MEP pathway	DXR1	Solyc03g114340	0.983938259	-0.082546381	0.410076944
MEP pathway	DXR2	Solyc06g060860	0.199524053	0.166352456	-0.292225453
MEP pathway	CMK	Solyc01g009010	0.884968181	0.014512289	0.480860925
MEP pathway	MCT	Solyc01g102820	0.488415714	0.40006911	0.364206591
MEP pathway	MDS	Solyc08g081570	0.213003447	0.122519655	0.623933883
MEP pathway	HDS	Solyc11g069380	0.882686457	0.057137735	0.423279789
MEP pathway	HDR	Solyc01g109300	-0.092325695	-0.444207896	-0.15767962
IPP isomerases	IDI1	Solyc08g075390	-0.053766114	-0.27002078	0.408431113
IPP isomerases	IDI2	Solyc05g055760	-0.01368272	0.152778807	0.657783139
IPP isomerases	IDI3	Solyc04g056390	0.29426506	-0.292380737	0.371964203
GGDR	GGDR1	Solyc01g088310	-0.130952114	0.708765564	-0.384847304
GGDR	GGDR2	Solyc03g115980	-0.396270784	0.152964101	-0.09490842
Tocopherol biosynthesis	HPPD1/PDS1a	Solyc05g041200	-0.003258982	-0.363823003	0.48259298
Tocopherol biosynthesis	HPPD2/PDS1b	Solyc07g045050	0.002860197	-0.071459139	-0.200460026
Tocopherol biosynthesis	VTE2	Solyc07g017770	0.553561893	0.064150277	0.381503736
Tocopherol biosynthesis	VTE3a	Solyc03g005230	0.424721351	0.110779221	0.105863188
Tocopherol biosynthesis	VTE3b	Solyc09g065730	0.228218686	0.081748204	0.610840864
Tocopherol biosynthesis	VTE1	Solyc08g068570	0.616813434	0.325744429	0.431115249
Tocopherol biosynthesis	VTE4a	Solyc08g076360	-0.151515162	0.236492581	0.506975932
Tocopherol biosynthesis	VTE4b	Solyc04g063230	-0.110780823	0.36361524	-0.302450315
Tocopherol biosynthesis	VTE4c	Solyc08g077240	-0.303071631	-0.145364926	-0.583830612
Tocopherol biosynthesis	VTE4d	Solyc03g116150	-0.290047454	-0.003146301	0.334972422
Chlorophyll biosynthesis	HEMA1	Solyc04g076870	-0.105259917	-0.274261136	0.419202338
Chlorophyll biosynthesis	HEMA2	Solyc01g106390	0.040718913	-0.159382416	0.72009636
Chlorophyll biosynthesis	HEMA3	Solyc01g089840	#N/A	#N/A	#N/A
Chlorophyll biosynthesis	GSA	Solyc04g009200	-0.082894254	-0.089319358	0.612747431
Chlorophyll biosynthesis	HEMB	Solyc08g069030	-0.151430238	-0.405537832	0.478103613
Chlorophyll biosynthesis	HEMC	Solyc07g066470	-0.071151521	0.459018759	0.129818671
Chlorophyll biosynthesis	HEMD	Solyc04g079320	0.469479524	-0.246514255	0.214036299
Chlorophyll biosynthesis	HEME1	Solyc10g007320	0.465700714	0.057792204	0.15566927
Chlorophyll biosynthesis	HEME2	Solyc06g048730	0.211799103	-0.094178477	0.065673668
Chlorophyll biosynthesis	HEMF	Solyc10g005110	0.665308945	0.044622375	0.339341703
Chlorophyll biosynthesis	HEMG1	Solyc01g079090	0.117133036	-0.407554853	0.350194089
Chlorophyll biosynthesis	HEMG2	Solyc03g005080	0.467537798	-0.369333515	0.659054874
Chlorophyll biosynthesis	CHLH	Solyc04g015750	-0.26701238	-0.110482093	-0.566896786
Chlorophyll biosynthesis	CHLI	Solyc10g008740	0.594459595	-0.038296053	-0.114544313
Chlorophyll biosynthesis	CHLD	Solyc04g015490	0.556081009	-0.167039536	0.183230703
Chlorophyll biosynthesis	CHLM	Solyc03g118240	0.458485616	0.400565799	0.182033019
Chlorophyll biosynthesis	CHL27-CRD	Solyc10g077040	-0.223630138	-0.00816874	-0.307798293
Chlorophyll biosynthesis	DVR	Solyc01g067290	-0.010768598	0.348905198	0.097673629
Chlorophyll biosynthesis	PORA	Solyc12g013710	-0.134290208	-0.112528933	0.241062199
Chlorophyll biosynthesis	PORB	Solyc07g054210	-0.196642498	-0.364421753	-0.136536604
Chlorophyll biosynthesis	PORC	Solyc10g006900	0.099037913	0.045790641	-0.121562843
Chlorophyll biosynthesis	CHLG1	Solyc05g024190	-0.162371852	0.001311095	0.31995561
Chlorophyll biosynthesis	CHLG2	Solyc09g014760	0.467429605	0.065746944	-0.1716427
Chlorophyll biosynthesis	CAOa	Solyc06g060310	-0.140415216	-0.307867459	-0.346880611
Chlorophyll biosynthesis	CAOb	Solyc11g012850	-0.134284865	-0.135540982	0.160700206
Chlorophyll degradation	CHL1	Solyc09g065620	#N/A	#N/A	#N/A
Chlorophyll degradation	CHL2a	Solyc06g053980	0.135263552	0.414254359	-0.090432445
Chlorophyll degradation	CHL2b	Solyc09g082600	-0.189527461	-0.431145721	-0.485581871
Chlorophyll degradation	CHL2c	Solyc12g005300	0.063207593	0.494543447	-0.189462652

Pathway/Family	Name	SOL Tomato gene	SIG1	SIG2	SIG3
			Solyc11g011240	Solyc04g079960	Solyc02g085700
Chlorophyll degradation	CLD1	Solyc02g070490	0.097418732	-0.019030447	-0.121496138
Chlorophyll degradation	SGR1	Solyc08g080090	0.334525535	0.351924964	0.239984752
Chlorophyll degradation	SGR2	Solyc12g056480	#N/A	#N/A	#N/A
Chlorophyll degradation	SGR3	Solyc04g063240	#N/A	#N/A	#N/A
Chlorophyll degradation	PPH	Solyc01g088090	-0.02570926	0.102250436	0.624178482
Chlorophyll degradation	PAO1	Solyc11g066440	0.075470096	-0.407248086	0.574465029
Chlorophyll degradation	PAO2	Solyc04g040160	#N/A	#N/A	#N/A
Chlorophyll degradation	PAO3	Solyc12g096550	-0.441818414	-0.426715473	-0.264975363
Chlorophyll degradation	RCCR	Solyc03g044470	0.252496332	-0.050336257	0.221137805
Chlorophyll degradation	PK1	Solyc03g071720	0.306310405	-0.274536284	0.638200534
Chlorophyll degradation	PK2	Solyc09g018510	-0.002769879	-0.124326081	-0.192384004
Chlorophyll degradation	NYC1	Solyc07g024000	0.079814353	-0.037916608	0.65448831
Chlorophyll degradation	CBR/NOL	Solyc05g032660	0.747124715	0.111886245	0.146036329
Chlorophyll degradation	HCAR	Solyc09g091100	-0.0128925	-0.289975445	-0.294073066
Phylloquinone biosynthesis	ICS1/MENF	Solyc06g071030	#N/A	#N/A	#N/A
Phylloquinone biosynthesis	PHYLLO/MEND1	Solyc04g005190	0.610474528	-0.184506979	0.118924512
Phylloquinone biosynthesis	PHYLLO/MEND2	Solyc04g005200	0.622287417	0.021210242	-0.02088809
Phylloquinone biosynthesis	PHYLLO/MEND3	Solyc04g005180	0.475484562	-0.108459214	0.163378551
Phylloquinone biosynthesis	AAE14	Solyc02g069920	0.06366328	0.073537116	-0.109614114
Phylloquinone biosynthesis	DHNS/MENB	Solyc05g005180	0.811508543	-0.001651354	0.216802597
Phylloquinone biosynthesis	DHNAT1	Solyc02g078410	-0.143053242	-0.125034472	0.501479632
Phylloquinone biosynthesis	DHNAT2	Solyc03g006440	#N/A	#N/A	#N/A
Phylloquinone biosynthesis	DHNAT3	Solyc03g006450	#N/A	#N/A	#N/A
Phylloquinone biosynthesis	ABC4	Solyc01g105460	0.45668733	0.076177322	0.606850632
Phylloquinone biosynthesis	MENG	Solyc12g019010	0.355667655	-0.429933867	-0.182348
Plastoquinone biosynthesis	TAT7/HPPS1	Solyc10g007110	-0.211383766	0.21345445	-0.302773187
Plastoquinone biosynthesis	TAT7/HPPS2	Solyc12g088000	-0.23856167	0.12907316	-0.477127228
Plastoquinone biosynthesis	TAT7/HPPS3	Solyc12g096240	-0.183757802	0.101931181	0.050024062
Plastoquinone biosynthesis	PDS2/HST	Solyc03g051810	0.449387501	-0.187413559	0.21955408
Plastoquinone biosynthesis	AAAT1	Solyc07g053720	-0.015951791	-0.366235433	0.43220791
Plastoquinone biosynthesis	AAAT2	Solyc10g008200	0.217492085	0.566893925	0.166994149
Plastoquinone biosynthesis	AAAT3	Solyc07g053710	0.17507915	0.196294288	0.588052247
Plastoquinone biosynthesis	ACS12	Solyc03g007070	-0.050853036	-0.291718623	-0.376091867
Plastoquinone biosynthesis	TAA1	Solyc05g031600	-0.259243414	-0.139275642	-0.375694205
Carotenoid biosynthesis	PSY1	Solyc03g031860	0.48436295	-0.068458482	0.183689089
Carotenoid biosynthesis	PSY2	Solyc02g081330	-0.372992877	0.255376259	-0.563151392
Carotenoid biosynthesis	PSY3	Solyc01g005940	0.9887403	-0.031173898	0.291125507
Carotenoid biosynthesis	PDS	Solyc03g123760	0.993379539	-0.045712605	0.322656275
Carotenoid biosynthesis	ZDS	Solyc01g097810	0.960459119	-0.021713467	0.302818591
Carotenoid biosynthesis	Z-ISO	Solyc12g098710	0.738619978	-0.091519099	0.551931703
Carotenoid biosynthesis	CRTISO1	Solyc10g081650	0.943765101	-0.100731764	0.464601885
Carotenoid biosynthesis	CRTISO2	Solyc05g010180	#N/A	#N/A	#N/A
Carotenoid biosynthesis	LCY-B1	Solyc04g040190	-0.060826955	0.034921071	0.126715816
Carotenoid biosynthesis	LCY-B2/CYC-B	Solyc10g079480	0.47083548	0.004718384	0.258287127
Carotenoid biosynthesis	LCY-E	Solyc12g008980	#N/A	#N/A	#N/A
Carotenoid biosynthesis	BCH1	Solyc06g036260	-0.494401783	-0.110140751	-0.278124838
Carotenoid biosynthesis	BCH2	Solyc03g007960	0.022206108	0.123623457	-0.182607406
Carotenoid biosynthesis	CYP97B3	Solyc05g016330	0.247342197	-0.15114203	-0.143317243
Carotenoid biosynthesis	CYP97A3	Solyc04g051190	0.934087572	0.079186798	0.433488572
Carotenoid biosynthesis	CYP97C1	Solyc10g083790	0.656435414	0.092000116	0.720760803
Carotenoid biosynthesis	ZEP1	Solyc06g060880	0.092497037	0.119284103	-0.356821625
Carotenoid biosynthesis	NSY1	Solyc02g089050	-0.141068334	0.150647962	-0.429764058
Carotenoid biosynthesis	VDE	Solyc04g050930	0.710345593	0.09745212	0.163692149
Carotenoid degradation	CCD1A	Solyc01g087250	0.897385096	-0.097410517	0.413828304
Carotenoid degradation	CCD1B	Solyc01g087260	-0.486507306	-0.319343808	0.12600825
Carotenoid degradation	CCDX	Solyc08g066720	0.962831828	0.005214157	0.244918912
Carotenoid degradation	CCD4A	Solyc08g075480	#N/A	#N/A	#N/A
Carotenoid degradation	CCD4B	Solyc08g075490	#N/A	#N/A	#N/A
Orange proteins	Or1	Solyc03g093830	0.956695311	-0.047672533	0.407062323
Orange proteins	Or2	Solyc09g010110	0.429020461	-0.375775452	0.375550783
ABA metabolism	NCED2	Solyc08g016720	0.877409595	0.007780788	0.427354139
ABA metabolism	NCED3	Solyc07g056570	0.471895819	0.112222671	0.570947911
ABA metabolism	NCED6	Solyc05g053530	#N/A	#N/A	#N/A

Pathway/Family	Name	SOL Tomato gene	SIG1	SIG2	SIG3
			Solyc11g011240	Solyc04g079960	Solyc02g085700
ABA metabolism	ABA2a	Solyc04g071940	0.028984238	0.338164225	-0.549218342
ABA metabolism	ABA2b	Solyc04g071960	#N/A	#N/A	#N/A
ABA metabolism	ABA2c	Solyc10g085380	-0.288588412	0.346337388	-0.511417212
ABA metabolism	ABA2d	Solyc11g018600	#N/A	#N/A	#N/A
ABA metabolism	AAO3a	Solyc11g065920	0.053296522	-0.464463544	0.571416643
ABA metabolism	AAO3b	Solyc11g065930	-0.22308611	0.03808593	0.499516268
ABA metabolism	ABA3	Solyc07g066480	0.498915173	0.063687929	0.200693733
ABA metabolism	ABA4	Solyc02g063170	-0.388641886	-0.152190581	-0.427829713
ABA metabolism	CYP707A1	Solyc04g078900	#N/A	#N/A	#N/A
ABA metabolism	CYP707A2	Solyc08g075320	0.121000641	-0.263589633	-0.418754624
ABA metabolism	CYP707A3a	Solyc01g108210	0.191959425	-0.166036381	0.502077133
ABA metabolism	CYP707A3b	Solyc08g005610	0.005129081	-0.321170606	-0.244657287
ABA metabolism	CYP707A3c	Solyc04g071150	0.911640177	-0.093816362	0.087467239
ABA metabolism	CYP707A3d	Solyc04g080650	-0.279642404	0.32164075	0.116087837
ABA metabolism	ABA1/ZEP	Solyc02g090890	-0.51934943	-0.030013217	-0.538058819
ABA metabolism	NSY3	Solyc02g086050	0.185788857	0.303292174	0.269656709
ABA metabolism	NSY5	Solyc06g074240	0.992272356	-0.075441014	0.340861095
SL biosynthesis	MAX3 (CCD7)	Solyc01g090660	0.992904154	-0.106902828	0.300371981
SL biosynthesis	MAX1	Solyc08g062950	0.986086882	-0.065425469	0.276445814
SL biosynthesis	MAX4 (CCD8)	Solyc08g066650	0.996596827	-0.059714661	0.297058985
Gibberellin metabolism	CPS1	Solyc06g084240	0.997400089	-0.102023381	0.306665528
Gibberellin metabolism	CPS2	Solyc08g005710	#N/A	#N/A	#N/A
Gibberellin metabolism	CPS3	Solyc09g065230	#N/A	#N/A	#N/A
Gibberellin metabolism	KS1a	Solyc07g066670	0.797763542	0.116676707	0.341005665
Gibberellin metabolism	KS1b	Solyc08g005720	0.45802595	0.427222273	-0.164064737
Gibberellin metabolism	KO	Solyc04g083160	0.99177426	-0.02644603	0.273361971
Gibberellin metabolism	KA01	Solyc01g080900	0.925218611	0.063463248	0.195364444
Gibberellin metabolism	KA02	Solyc08g007050	#N/A	#N/A	#N/A
Gibberellin metabolism	KA03	Solyc12g006460	-0.043884958	0.538148128	0.135522157
Gibberellin metabolism	KA04	Solyc10g007860	#N/A	#N/A	#N/A
Gibberellin metabolism	GA20ox1	Solyc03g006880	0.990700671	-0.061266037	0.279604246
Gibberellin metabolism	GA20ox2	Solyc09g009110	#N/A	#N/A	#N/A
Gibberellin metabolism	GA20ox3	Solyc11g072310	0.764067607	0.079907645	0.030099693
Gibberellin metabolism	GA20ox4	Solyc06g035530	#N/A	#N/A	#N/A
Gibberellin metabolism	GA20ox5	Solyc01g093980	0.979136723	-0.070374827	0.274557014
Gibberellin metabolism	GA20ox6	Solyc06g050110	#N/A	#N/A	#N/A
Gibberellin metabolism	GA20ox7	Solyc11g013360	#N/A	#N/A	#N/A
Gibberellin metabolism	GA3ox1	Solyc06g066820	0.97438317	-0.042467304	0.262767095
Gibberellin metabolism	GA3ox2	Solyc03g119910	#N/A	#N/A	#N/A
Gibberellin metabolism	GA3ox3	Solyc00g007180	#N/A	#N/A	#N/A
Gibberellin metabolism	GA3ox4	Solyc01g058250	-0.158328167	-0.133515069	0.596201491
Gibberellin metabolism	GA3ox5	Solyc05g052740	#N/A	#N/A	#N/A
MVA pathway	HMG51	Solyc08g080160	#N/A	#N/A	#N/A
MVA pathway	HMG52	Solyc08g007790	-0.082203011	-0.171648603	0.636394447
MVA pathway	HMG53	Solyc12g056450	0.108375307	-0.083799696	-0.282527204
MVA pathway	HMG54	Solyc08g080170	-0.119184485	0.064018582	0.67219755
MVA pathway	HMGR1	Solyc03g032020	0.233838251	-0.269895899	0.493862077
MVA pathway	HMGR2	Solyc02g082260	-0.243850449	-0.482597207	-0.321043725
MVA pathway	HMGR3	Solyc02g038740	-0.08065974	-0.159039759	0.64130647
MVA pathway	HMGR4	Solyc03g032010	0.448026273	0.140362687	0.252487654
MVA pathway	MVK	Solyc01g098840	-0.101188848	-0.192849616	0.63006538
MVA pathway	PMK1	Solyc08g076140	0.118637298	-0.392787149	0.587969204
MVA pathway	PMK2	Solyc06g066310	0.063436412	-0.060619985	0.729922806
MVA pathway	MVD1	Solyc04g009650	0.028841528	0.197760815	0.612150651
MVA pathway	MVD2	Solyc11g007020	-0.120558081	-0.097527905	0.629381981
MVA pathway	AACT1	Solyc05g017760	0.185899173	0.615360485	0.347271304
MVA pathway	AACT2	Solyc07g045350	-0.108831687	-0.122710038	0.650776949
MVA pathway	AACT3	Solyc04g015100	0.088470241	0.04828122	0.728496447
FDS	FDS1	Solyc10g005840	0.523849783	-0.102281461	0.102421253
FDS	FDS2	Solyc12g015860	-0.079504135	-0.031898035	0.637541783
FDS	FDS3	Solyc10g005810	0.4018755	0.248462877	0.32880738
FDS	FDS4	Solyc10g005820	0.375810018	0.419812374	0.253962811
Ubiquinone biosynthesis	PPT1	Solyc03g114300	0.388805365	-0.095730347	0.673083897
Ubiquinone biosynthesis	CoQ3	Solyc07g055850	0.43200067	0.35963032	0.07331323
Ubiquinone biosynthesis	CoQ5a	Solyc01g081470	0.074871819	0.06013107	0.559041736
Ubiquinone biosynthesis	CoQ6	Solyc09g091570	0.68029036	-0.227989585	0.196851133

SUPPORTING REFERENCES

- Barja, M. V., Ezquerro, M., Beretta, S., Diretto, G., Florez-Sarasa, I., Feixes, E., Fiore, A., Karlova, R., Fernie, A. R., Beekwilder, J., & Rodríguez-Concepción, M. (2021). Several geranylgeranyl diphosphate synthase isoforms supply metabolic substrates for carotenoid biosynthesis in tomato. *New Phytologist*, 231(1), 255–272.
- Barja, M. V., & Rodriguez-Concepcion, M. (2020). A Simple In Vitro Assay to Measure the Activity of Geranylgeranyl Diphosphate Synthase and Other Short-Chain Prenyltransferases. *Methods in Molecular Biology*, 2083: 27-38
- Ezquerro, M., Burbano, E., & Rodríguez-Concepción, M. (2022) Overlapping and specialized roles of tomato phytoene synthase isoforms PSY1 and PSY2 in carotenoid and ABA production. *bioRxiv* doi: 10.1101/2022.08.11.503628.
- Floková, K., Tarkowská, D., Miersch, O., Strnad, M., Wasternack, C., & Novák, O. (2014). UHPLC–MS/MS based target profiling of stress-induced phytohormones. *Phytochemistry*, 105, 147-157.
- Kohlen, W., López Ráez, J.A., & Bouwmeester H.J. (2012). Tomato strigolactones: a more detailed look. *Plant, Signalling & Behavior* 8: e22785
- López-Gresa, M. P., Lisón, P., Campos, L., Rodrigo, I., Rambla, J. L., Granell, A., Conejero, V., & Bellés, J. M. (2017). A non-targeted metabolomics approach unravels the VOCs associated with the tomato immune response against *Pseudomonas syringae*. *Frontiers in Plant Science*, 8, 1188-1199.
- Simon, P. (2003). Q-Gene: Processing quantitative real-time RT-PCR data. *Bioinformatics*, 19(11), 1439–1440.
- Wang, Y., Duran, H. G. S., van Haarst, J. C., Schijlen, E. G., Ruyter-Spira, C., Medema, M. H., Dong, L., & Bouwmeester, H. J. (2021). The role of strigolactones in P deficiency induced transcriptional changes in tomato roots. *BMC plant biology*, 21(1), 1-21.
- Wang, Y., Durairaj, J., Duran, H. G. S, van Velzen, R., Flokova, K., Liao, C. Y., Chojnacka, A., MacFarlane, S., Schranz, M. E., Medema, M. H., van Dijk, A. D. J., Dong, L., & Bouwmeester, H. J. (2022). The tomato cytochrome P450 CYP712G1 catalyses the double oxidation of orobanchol en route to the rhizosphere signalling strigolactone, solanacol. *New Phytologist* 235(5), 1884-1899.
- Xie, X.N., Yoneyama, K., Kurita, J.Y., Harada, Y., Yamada, Y., Takeuchi, Y., & Yoneyama, K. (2009) 7-Oxo-orobanchyl acetate and 7-Oxo-orobanchol as germination stimulants for root parasitic plants from flax (*Linum usitatissimum*). *Bioscience Biotechnology Biochemistry* 73(6): 1367-1370.

Zhang, Y., van Dijk, A. D. J., Scaffidi, A., Flematti, G. R., Hofmann, M., Charnikhova, T., Verstappen, F., Hepworth, J., van der Krol, S., Leyser, O., Smith, S. M., Zwanenburg, B., Al-Babili, S., Ruyter-Spira, C., & Bouwmeester, H. J. (2014). Rice cytochrome P450 MAX1 homologs catalyze distinct steps in strigolactone biosynthesis. *Nature Chemical Biology*, 10(12), 1028–1033.

Zhang, Y., Cheng, X., Wang, Y., Díez-Simón, C., Flokova, K., Bimbo, A., Bouwmeester, H.J., & Ruyter-Spira, C. (2018) The tomato MAX1 homolog, SIMAX1, is involved in the biosynthesis of tomato strigolactones from carlactone. *New Phytologist* 219(1): 297-309.